

FULL FIELD X-RAY FLUORESCENCE IMAGING USING MICRO PORE OPTICS FOR PLANETARY SURFACE EXPLORATION.

Philippe Sarrazin	SETI Institute, Mountain View, CA 94043
David Blake	NASA Ames Research Center, Moffett Field, CA 94035
Marc Gailhanou	CNRS, IM2NP UMR, Marseille, France
Philippe Walter	Sorbonne Universités, CNRS-UPMC, LAMS, Paris, France
Emile Schyns	PHOTONIS France SAS, Avenue Roger Roncier, 19100 Brive, France
Franck Marchis	SETI Institute, Mountain View, CA 94043
Kathy Thompson	SETI Institute, Mountain View, CA 94043
Thomas Bristow	NASA Ames Research Center, Moffett Field, CA 94035

Many planetary surface processes leave evidence as small features in the sub-millimetre scale. Current planetary X-ray fluorescence spectrometers lack the spatial resolution to analyse such small features as they only provide global analyses of areas $>100 \text{ mm}^2$. A micro-XRF spectrometer will be deployed on the NASA Mars 2020 rover to analyse spots as small as $120 \mu\text{m}$. When using its line-scanning capacity combined to perpendicular scanning by the rover arm, elemental maps can be generated.

We present a new instrument that provides full-field XRF imaging, alleviating the need for precise positioning and scanning mechanisms. The Mapping X-ray Fluorescence Spectrometer - "Map-X" - will allow elemental imaging with $\sim 100 \mu\text{m}$ spatial resolution and simultaneously provide elemental chemistry at the scale where many relevant physical, chemical and biological features can be imaged in ancient rocks.

The arm-mounted Map-X instrument is placed directly on the surface of an object and held in a fixed position during measurements. A $25 \times 25 \text{ mm}^2$ surface area is uniformly illuminated with X-rays or α -particles and γ -rays. A novel Micro Pore Optic focusses a fraction of the emitted X-ray fluorescence onto a CCD operated at a few frames per second. On board processing allows measuring the energy and coordinates of each X-ray photon collected. Large sets of frames are reduced into 2d histograms used to compute higher level data products such as elemental maps and XRF spectra from selected regions of interest. XRF spectra are processed on the ground to further determine quantitative elemental compositions.

The instrument development will be presented with an emphasis on the characterization and modelling of the X-ray focussing Micro Pore Optic. An outlook on possible alternative XRF imaging applications will be discussed.

FULL FIELD X-RAY FLUORESCENCE IMAGING USING MICRO PORE OPTICS FOR PLANETARY SURFACE EXPLORATION

P. Sarrazin¹, D. F. Blake², M. Gailhanou³, P. Walter⁴, E. Schyns⁵, F. Marchis¹, K. Thompson¹, T. Bristow²
¹SETI Institute, Mountain View, CA 94043, USA, psarrazin@seti.org, ²NASA Ames Research Center, Moffett Field, CA 94035 USA, david.blake@nasa.gov, ³Aix-Marseille Univ., CNRS, IM2NP, Marseille, France, ⁴Sorbonne Universités, CNRS-UPMC, LAMS, Paris, France, ⁵PHOTONIS France SAS, Avenue Roger Roncier, 19100 Brive, France

I INTRODUCTION

Many planetary surface processes leave evidence as small features in the sub-millimetre scale. Current planetary X-ray fluorescence spectrometers lack the spatial resolution to analyze such small features as they only provide global analyses of areas $>100 \text{ mm}^2$. A micro-XRF spectrometer will be deployed on the NASA Mars 2020 rover to analyze spots as small as $120 \mu\text{m}$. When using its line-scanning capacity combined to perpendicular scanning by the rover arm, elemental maps can be generated. We present an instrument that provides full-field XRF imaging, alleviating the need for precise positioning and scanning mechanisms. The Mapping X-ray Fluorescence Spectrometer (MapX) will allow elemental imaging with $\sim 100 \mu\text{m}$ spatial resolution and simultaneously provide elemental chemistry at the scale where many relict physical, chemical and biological features can be imaged in ancient rocks. The arm-mounted MapX instrument is placed directly on the surface of an object and held in a fixed position during measurements. A $25 \times 25 \text{ mm}^2$ surface area is uniformly illuminated with X-rays or γ -rays and α -particles. A Micro Pore Optic focuses a fraction of the emitted X-ray fluorescence onto a CCD operated in single photon counting mode over thousands of short acquisitions. On board processing allows a measurement of both the energy and coordinates of each X-ray photon collected. Large sets of frames are reduced into 2d histograms used to compute higher level data products such as elemental maps and XRF spectra from selected regions of interest. XRF spectra are processed on the ground to further determine quantitative elemental compositions.

II SCIENCE OBJECTIVES

Many planetary surface processes (like physical, chemical and energetic particle (space) weathering; water activity; diagenesis; low-temperature or impact metamorphism; and biogenic activity) leave traces as features in the size range 10s to 100s of μm . These features can be either laterally oriented (veins or mineral grains in a rock) or vertically oriented (space or atmospheric weathering rinds and coatings). Such features can be compositional (surface leaching or deposition of elements, growth of secondary phases, veining, biominerals or biofabrics, surface-atmosphere, energetic particle interaction), morphological (dissolution features, fracture surfaces, biominerals or biofabrics, secondary phases such as clays/carbonates, crystal shapes, veining or pitting), or mineralogical (characteristic solid phases or associations of phases).

For identifying these diagnostic features, it is critically important to acquire elemental compositional information at length scales that are less than or equal to the dimensions of grains, phases, or features being imaged or analyzed. For example, if a rock contains mineral grains that are on the order of $\sim 100 \mu\text{m}$, elemental analyses of larger volumes of material are not definitive with regard to mineralogy or provenance as they will represent mixtures. Does a rock contain veins, exsolution features, or secondary phases? Are adjacent phases in thermodynamic equilibrium based on their chemical compositions and inferred mineralogy?

MapX will provide elemental maps and quantitative XRF spectra from Regions of Interest (ROIs) having a spatial resolution commensurate with optical images, invaluable for elucidating fine-scale sedimentary petrology and low-temperature diagenesis in ancient Mars rocks and other planetary surfaces.

III INSTRUMENT DESCRIPTION

MapX is an arm-deployed full-field X-ray spectrometer placed directly on a surface to be analyzed and held there by contact pads/sensors during an analysis. The instrument will collect $2.5 \times 2.5 \text{ cm}$ elemental images with $\sim 100 \mu\text{m}$ spatial resolution, recording the compositions of individual mineral grains, primary petrologic fabrics, vein fillings, and other depositional and diagenetic features on a scale length commensurate with other arm-based imaging instruments.

The principal components of MapX are shown in Fig. 1. The sample surface is irradiated by X-rays, γ -rays, or α -particles from sources on the instrument head (both electrical and radioisotope sources are evaluated). Fluoresced X-rays emitted in the direction of an X-ray sensitive CCD pass through an X-ray 1:1 focusing lens called a Micro Pore Optic (MPO) [1] that projects a spatially resolved image of the X-rays generated from the sample surface onto the CCD. A single analysis comprises $\sim 10,000$ raw images over a $\sim 10,000$ second period. Higher-level data products obtained from the raw images include single-element maps and XRF spectra from ground-selected or instrument-selected ROIs that can be processed to determine quantitative elemental abundances.

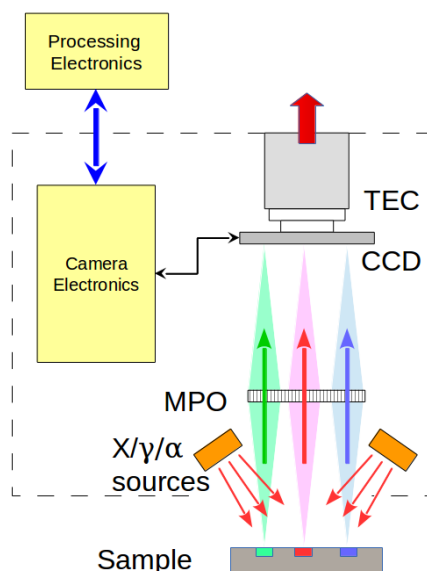


Fig. 1: Principal components of MapX: X/γ/α source illuminates the surface of the sample, fluoresced X-rays pass through a Multi Pore Optic (MPO) and are focused on the Charge Couple Device (CCD) detector, in direct detection, cooled by a multistage Peltier Thermo Electric Cooler (TEC)

III-A X-ray fluorescence spectrometry

Of the techniques used to determine elemental chemistry on remote planetary surfaces, XRF (or APXS or PIXE when α -particles are used as the excitation source) is the most direct and unequivocal because the technique is based on well-known principles of atomic physics and has been used for decades on Earth and in spaceflight missions. Elements useful in interpreting the fine-scale petrology of rocks include Na, Mg, Al, Si, P, S, Cl, K, Ca, Ti, Cr, Mn, and Fe and higher. For these elements, X-rays originating from the K shell are most useful, having detectable energies from 1.04 KeV (Na K α) to 11.904 (Br K α).

On Mars, XRF instruments have used radioisotope sources (APXS, ^{244}Cm), and X-ray tube sources (CheMin, Co K α). The latter requires a high-voltage power supply (HVPS) and X-ray tube, and control electronics. Decreases in mass, power, and complexity are realized when radioisotope sources are used for arm-based XRF instrumentation, as is the case for APXS. We are developing and evaluating both X-ray tubes and radioisotopes as fluorescing sources for MapX.

III-B X-ray image formation

Most current XRF mapping instruments (commercial systems, synchrotron based instruments and the Mars 2020 PIXL instrument) rely on scanning a focused X-ray beam in x and y across the surface of the sample analyzed. MapX uses a Full-Field XRF (FF-XRF) imaging approach to image the entire surface in parallel, alleviating the requirement for precise scanning. FF-XRF systems have been demonstrated -including by our own initial studies- using a pinhole layout similar to early “camera obscura” photographic instruments [2], but offer low throughput due to the small aperture required to achieve an acceptable resolution. Glass polycapillary optics based FF-XRF have been developed [3], using similar imaging principle as fiber optic couplers, resolution and throughput are driven by the limited acceptance angle of capillaries. MapX uses an X-ray focusing optic to allow good resolution and increased throughput. X-ray focusing lenses rely on reflection at grazing incidence (under the critical angle, typically a few tenths to a few degrees depending on X-ray energy and surface material). The Micro Pore Optic (MPO) (Fig. 2) used in MapX is a multichannel reflective X-ray lens composed of an array of microscopic square-section channels whose walls act as imaging mirrors similar to Kirkpatrick-Baez mirror pairs [4]. X-rays that enter the optic at angles to a channel axis no higher than the critical angle will either pass through the channel or be submitted to one or a series of reflections with the

channel walls. Depending on the number and types of reflections, X-rays are partially or completely focused on the image plane. Also known as “Lobster-eye” optics because of the similarity of their operation with that of crustacean eyes, these optics are used in X-ray astronomy [1], typically in a doubly curved geometry. MapX uses a simpler flat geometry for 1:1 focusing, as described in [5].

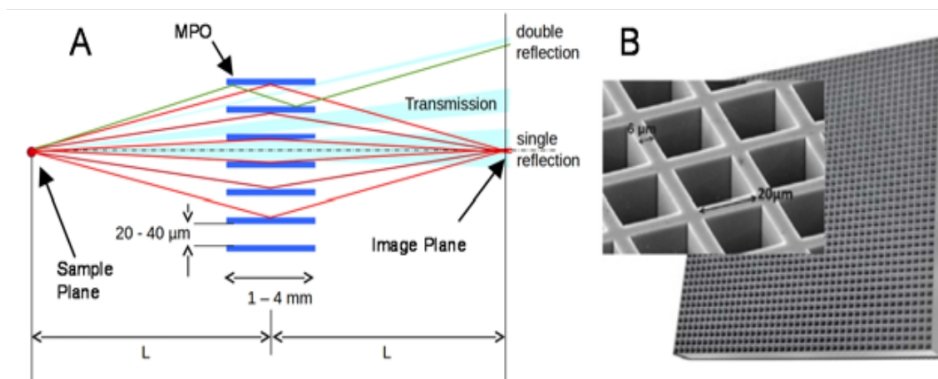


Fig. 2: Micro Pore Optics (MPO) used in MapX for 1:1 focusing of the X-ray fluorescence signal emitted by the sample; A: 2D representation of transmitted and reflected X-rays; B: SEM image of an MPO showing the entrance of the channels (20μm wide, 6μm walls)

III-C X-ray detection

An X-ray sensitive CCD imager directly detects X-rays fluoresced from the sample. The imager is operated in single-photon counting mode, i.e., the CCD is exposed and read often enough that nearly all pixels record either the charge deposited by a single X-ray photon added to their dark current accumulation, or only the dark current accumulation representing no incident photons. When an X-ray photon is absorbed into a single x,y pixel of the CCD, the photon energy is deposited in the volume of the pixel as electron-hole pairs, each of which represents ~3.65 eV of energy. The energies of X-ray photons from elements of biological or geological interest range from a few hundred to many thousands of eV. For example, a single Ca K α X-ray photon fluoresced from the sample has an energy of 3.68 keV, and deposits 1,008 electrons into a single x,y pixel of the CCD. During a full analysis of a sample, the CCD detector is exposed to the X-ray photon flux from the sample, read out, and erased many times. This method was used for the CheMin instrument on MSL [6] that has been operated successfully on Mars for nearly 4 years. In MapX, data from each exposure are stored and processed in real time so that over time, high-spatial resolution elemental maps and XRF spectra from selected ROIs can be acquired.

III-D Data Processing

MapX collects a large number of short acquisitions that are combined into x-y-time data cubes. Python code was developed for processing raw CCD data from the prototype instruments. The code includes background correction, split charge removal, and optional binning features. The resulting x-y-energy data cubes are stored in HDF5 format and analyzed using the open source program PyMca [7] for construction of elemental maps, selection of spatial or spectral regions of interest, and quantitative analysis with fundamental parameter methods. The spectral data cubes files are large and incompatible with the limited bandwidth of planetary missions. Additional on-board processing to further reduce data into alternative products such as element maps, XRF spectra of ROIs or x,y maps of spectral ROIs will be developed for the flight instrument.

III-E Radioisotope source development

Theoretical models are being developed for X/ γ -ray source emission and X-ray fluorescence response of the sample to guarantee sufficient flux to meet elemental detection limits for selected minor elements and elemental accuracy/precision limits for major elements. A combination of empirical measurements and modeling using the Monte Carlo programs XMIMSIM [8] and PyMca [7] are used to determine X-ray tube and radioisotope source requirements. A model of α -particle fluorescence is developed using the open source program GEANT4 [9].

IV FLIGHT IMPLEMENTATION

MapX will be an arm-based instrument placed on the surface of an object to be analyzed and held in registry with it through the use of sensors that physically touch the surface. MapX will be operated at night and during times of the day when active cooling with a thermoelectric cooler (TEC) can lower the CCD temperature to -40°C or below. The instrument consists of two units: an Arm Unit that carries the camera head electronics and excitation sources (either X-ray tube or radioisotope based), and a Rover Avionics Mounting Platform (RAMP) Unit that controls and powers the Arm unit, processes X-ray data and communicates with the Rover Compute Element. Fig. 3 shows a preliminary design of the Arm Unit, including touch sensors, a 1-time operable

instrument cover, excitation sources (X-ray tube [left] or ^{244}Cm radioisotope [right]), an X-ray Micro-Pore Optic (MPO) lens, a CCD with active cooling via TEC, and the camera head electronics.

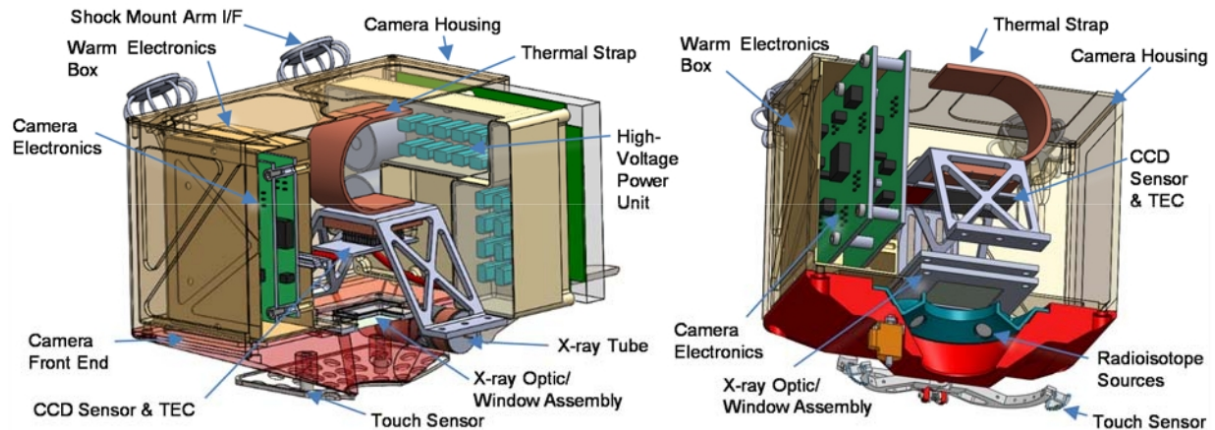


Fig. 3: Preliminary designs of two flight configurations of the MapX Arm Unit:
Left: X-ray tube source based design, Right: more compact radioisotope based design.

V MAPX DEVELOPMENT PROTOTYPES

MapX development resulted in prototypes and test fixtures that demonstrated proof-of-concept for the MapX instrument. A first instrument (MapX-I) based on components from a portable XRD system was used to validate the MapX principle, but had limited functionality relative to the proposed flight instrument. The design and early results from the instrument are presented in [10-11]. A second prototype (MapX-II) was built from commercial components and specialized software (Fig. 4). It is based on an commercial camera (Andor iKon M) with a 1024×1024 back-illuminated deep-depletion CCD kept under a sealed vacuum with a $200\mu\text{m}$ thick Be window. A Peltier cooler maintains the CCD at -60 to -80°C during operation to limit dark current. Two transmission target X-ray tubes (Moxtek Magnum 40kV-4W Au) illuminate the sample from opposite sides of the camera to limit topographic contrast. An MPO sourced from an existing batch at PHOTONIS is placed equidistant between the sample plane and the CCD (50mm distance). The 1Mhz readout of the camera allows the instrument to be driven at about 2 frames/sec when 2×2 binning is used. The X-ray sources are shuttered during read cycles to prevent CCD exposure during readout shifts. A parallel development based on the same design resulted in Cartix, a full-field XRF instrument used in Cultural Heritage research [12].

A new prototype (MapX-III), currently in assembly, is intended to be a more flight-like configuration of MapX. It uses the E2V CCD224 developed for the MSL CheMin XRD instrument and based on the CCD22 used in X-ray space telescopes (XMM-Newton EPIC [13], and Swift XRT [14]). The CCD224 is a frame-transfer device, allowing nearly instantaneous transfer of an acquired frame of data into a storage frame masked from the incoming radiation. The stored frame can then be read at reasonably slow readout rate (500 kHz) while the next frame is acquired. The frame transfer architecture enables high duty cycles compared to a full-frame device, and alleviates the need for a shutter. The CCD will be operated at $\sim 1\text{ fps}$ to ensure a low density of detected photons between frame transfers, allowing for single-photon counting and proper discrimination of event types. The custom camera of MapX-III is directly bolted to a vacuum chamber containing the MPO, X-ray tubes and a sample carousel. The custom camera electronics remains outside the vacuum. This instrument will be used to evaluate overall performance of the eventual flight system, characterize candidate MPOs, optimize instrument geometry and develop data collection and reduction software.

VI CHARACTERIZATION AND MODELING OF MPO FOCUSING

VI-A Ray tracing model of the MPO

A theoretical model of the MPO was developed and simulations of MapX were obtained by ray tracing. Discrepancies between initial simulations and MapX-II data revealed the effect of a non-perfect geometry of the MPO. In collaboration with the MPO manufacturer PHOTONIS, the MPO manufacturing process [15] was examined to assess the possible resulting defects in the MPO geometry. Implementation of defects in the MPO model (stacking error, angular error, twist, etc.) has been initiated.

The spatial resolution of MapX is driven by the structured signal spread that is produced by the MPO, visible in particular in elemental images obtained with MapX-II (Fig. 5.). Comparison of MapX-I and MapX-II data,

along with recent simulation results, pointed to a degradation of the resolution from the increased optic-detector distance (35mm for MapX-I, 50mm for MapX-II). Shorter distances will be used in MapX-III.

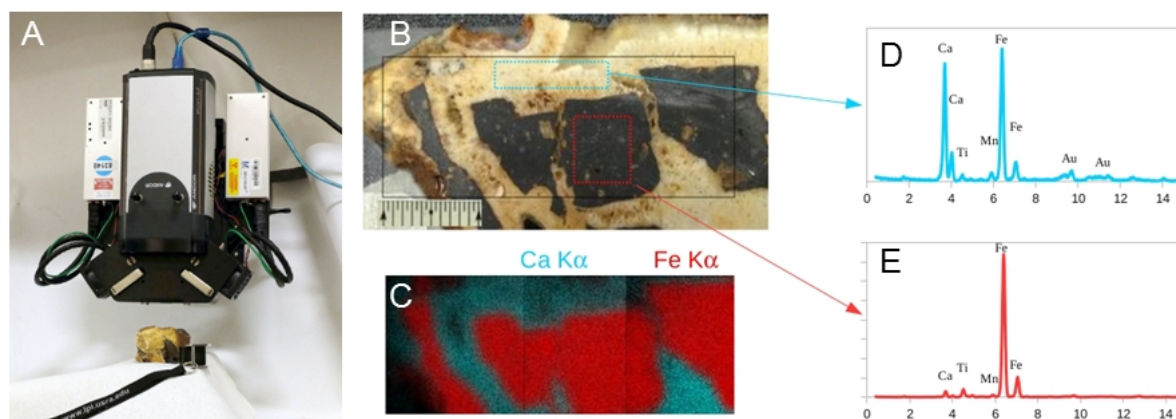


Fig. 4: MapX-II prototype. A) instrument in position to analyze a rock sample. B) Optical image of sample composed of breccia fragments and light-toned cement (scale is in mm). C) Fe K α / Ca K α map obtained by tiling 3 analyses of 1000s integration. D&E) XRF spectra of two ROIs

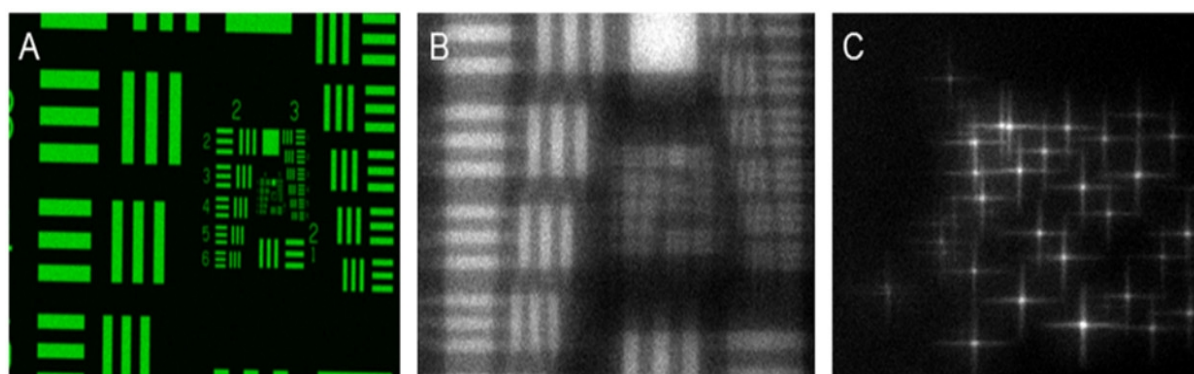


Fig. 5: Resolution test of MapX-II. USAF 1951 imaging standard, Cr on Glass. A) Cr image obtained in a commercial EDAX Orbis PC instrument with a 30 μ m polycapillary optic (\sim 80 μ m resolution). B) Raw Cr map measured with the MapX-II instrument. Resolution is decreased as a result of the MPO lens PSF. C) Raw Fe map of 60 μ m Fe particles with the MapX-II instrument. The Fe particles that appear as crosses, in which photon intensity is spread away from the source particles in x and y directions.

VI-B Measurement of the Point Spread function at SSRL

A 24-hr beam access to Stanford synchrotron beam-line (SSRL BL2-3) allowed direct measurement of the Point Spread Function (PSF) of our current MPOs. BL2-3 allows less than 10 μ m spot illumination of a thin metallic foil, providing an emission spot over one order-of-magnitude smaller than the MapX target resolution. This source is practically considered as a point source and allows direct measurement of the PSF using either a MapX prototype or a dedicated setup with MPO and CCD camera. PSF measurements were carried out at different energies, distances, and positions on the MPO. The observed PSFs are compared to computed PSF using the ray tracing simulations (Fig. 6).

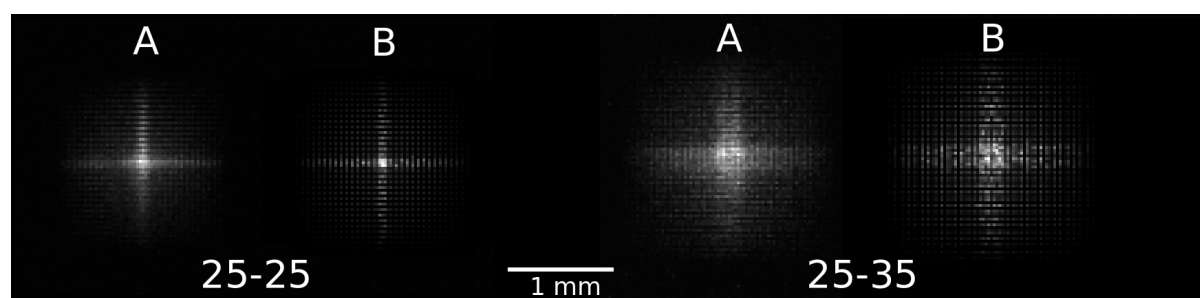


Fig. 6: Comparison of PSF data collected at SSRL BL2-3 (A) and obtained by ray tracing simulations (B) at a nominal CCD-MPO distance of 25 mm and 7.5 keV energy (Ni K α). Left: sample in focus (25-25); Right: sample out of focus by 10mm (25-35) resulting in a loss of resolution of \sim 100 μ m.

VI-C MPO design optimization

A planned task toward improving the imaging performance of MapX is to optimize the MPO lens for 1:1 imaging. Lens thickness, channel size and internal coating are the main parameters that can be adjusted in the MPO design. Key to this optimization is the continuing effort to model and characterize MPO lenses and simulate their operation with ray tracing. The characterization of MPOs will be conducted by testing in the MapX-III instrument, and PSF measurements at the Stanford synchrotron (SSRL BL2-3).

VI-D Deconvolution of MPO point spread function

In parallel with minimizing the PSF via MPO and instrument design optimization, an effort has been engaged to develop software for deconvolution of the PSF from experimental MapX data. A computer code based on the AIDA deconvolution algorithm [16] has been developed to enhance the resolution of MapX data. Preliminary results are shown in Fig. 7, yielding a resolution of 135 μm after deconvolution.

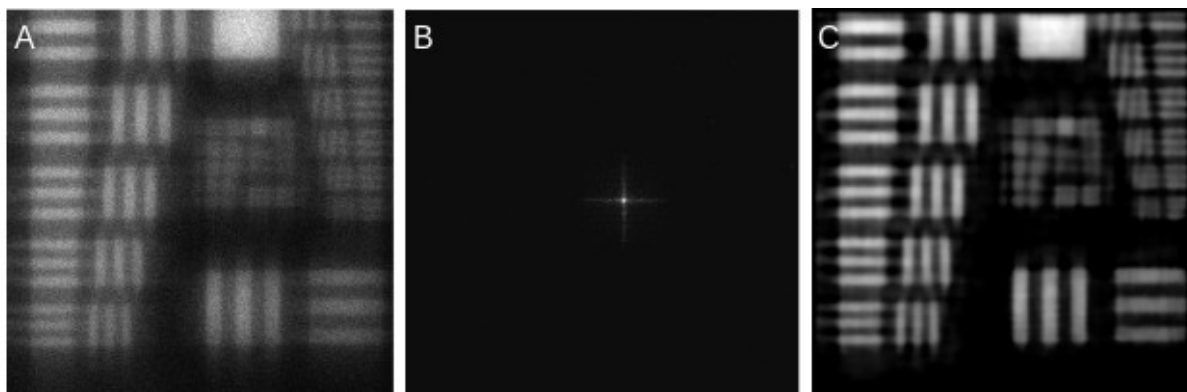


Fig. 7: MapX PSF Deconvolution Example. A) Original image. Chromium $K\alpha$ X-rays (5.4 keV) taken with MapX-II (MPO-CCD = MPO-Target = 50 mm). The resolution of this image is estimated to be 200 μm . B) Point Spread Function measured at the Stanford synchrotron (FWHM $\sim 165 \mu\text{m}$). C) AIDA deconvolution with automatized cost function parameters (resolution $\sim 135 \mu\text{m}$).

VIII CONCLUSION

MapX is a Full Field XRF instrument developed for future landed planetary missions. It will be installed on a robotic arm and placed in contact with the rock surface to be analyzed. The instrument concept relies on a 1:1 imaging Micro-Pore Optic to form an image on the CCD detector. Unlike other mapping XRF system, MapX does not require precision scanning of the instrument or a microfocused beam to compose an image of the sample. The instrument concept has been demonstrated in the laboratory. Field demonstration of prototypes in Mars analog sites is planned for 2017. In parallel of the concept development, major efforts have been placed in the design of high Technical Readiness Level (TRL) subsystems such as CCD detector, camera electronics, X-ray source, radioisotope sources, etc. MapX is currently developed to TRL-4 and detailed plans have been put in place to increase the instrument to TRL-6.

ACKNOWLEDGEMENTS

The authors wish to thank NASA Ames Research Center for the initial funding under the Center Innovation Fund, the NASA PICASSO program for funding the current development, SLAC for providing beam time at the Stanford Synchrotron Light Source BL2-3, and C. Chalumeau and S. Gavino for their contributions to this work during their internships.

REFERENCES

- [1] Fraser, G.W. et al. (2010). "The mercury imaging X-ray spectrometer (MIXS) on bepicolombo." *Planet. Space Sci.* 58 (1-2), 79-95.
- [2] M.G. Vasin, Y.V. Ignatiev, A.E. Lakhtikov, A.P. Morovov, V.V. Nazarov; "Energy-resolved x-ray imaging", *Spectrochim. Acta Part B*, 62 (2007), pp. 648–653
- [3] Bjeoumikhov, A., G. Buzanich, N. Langhoff, I. Ordavo, M. Radtke, U. Reinholz, H. Riesemeier, O. Scharf, H. Soltauc and R. Wedelle (2012). "The SLcam: a full field energy dispersive X-ray camera." 14th

- International Workshop on Radiation Imaging Detectors, 1-5 July 2012, Figueira da Foz, Portugal. doi:10.1088/1748-0221/7/11/C11008.
- [4] Kirkpatrick P. and A. V. Baez (1948). "Formation of Optical Images by X-rays." *J. Opt. Soc. Am.* 38:766-774
- [5] G.J. Price et al. (2004). "Prototype imaging x-ray fluorescence spectrometer based on microchannel plate optics." *Rev. Sci. Inst.*, Vol. 75 No. 7, doi: 10.1063/1.1764610.
- [6] David Blake, David Vaniman, Cherie Achilles, Robert Anderson, David Bish, Tom Bristow, and 18 others (2012). "Characterization and Calibration of the CheMin Mineralogical Instrument on Mars Science Laboratory." *Space Science Reviews*, Vol. 170, Issue 1-4, pp. 341-399.
- [7] V.A. Solé et al. (2007). "A multiplatform code for the analysis of energy-dispersive X-ray fluorescence spectra." *Spectrochim. Acta Part B*, 62, 63-68.
- [8] Schoonjans T. et al. (2012) "The xraylib library for X-ray-matter interactions. Recent developments." *Spectrochim. Acta Part B*, 70, 10-23.
- [9] Mantero, A., H. Ben Abdelouahed, C. Champion, Z. El Bitar, Z. Francis, P. Gueye, S. Incerti, V. Ivanchenko and M. Maire (2011). "PIXE simulation in Geant4." (wileyonlinelibrary.com) DOI 10.1002/xrs.1301.
- [10] Blake, D.F., P. Sarrazin and T. Bristow (2014). "Mapping a-particle X-ray Fluorescence Spectrometer (Map-X)." *IPM-2014*, #1080.
- [11] Blake, D.F., P. Sarrazin and T. Bristow (2015). "Mapping X-ray Fluorescence Spectrometer (Map-X)." *LPSC XLVI Abstr.* #2274
- [12] Walter, P., P. Sarrazin, D. Blake, M. Gailhanou, D. Hérouard and A. Verney (2016). "A new in-situ X-ray fluorescence full field imaging instrument revealing new insights on Impressionists' techniques." Unpublished
- [13] Struder, L., et al., (2001). "The European Photon Imaging Camera on XMM-Newton: The pn-CCD Camera." *Astronomy and Astrophysics*, 365, L18.
- [14] Burrows et al., (2005). "The Swift X-ray Telescope." *Spac Sci. Rev.* 120,:165, 2005.
- [15] J.L. Mutz, O. Bonnet, R. Fairbend, E. Schyns, J. Seguy. (2007). "Micro-pore optics: from planetary X-Rays to industrial market, Quantum Sensing and Nanophotonic Devices IV", edited by Manijeh Razeghi, Gail J. Brown, *Proc. of SPIE Vol. 6479*, 64790F, (2007).
- [16] Hom, E.F.Y. et al., (2007). "AIDA: an adaptive image deconvolution algorithm with application to multi-frame and three-dimensional data." *Journal of the Optical Society of America. A, Optics, image science, and vision*, 24(6), pp.1580–600. Available at: <http://www.ncbi.nlm.nih.gov/pubmed/17491626>.